Bioorganic & Medicinal Chemistry Letters 27 (2017) 5230–5234

Contents lists available at ScienceDirect

Bioorganic & Medicinal Chemistry Letters

journal homepage: www.elsevier.com/locate/bmcl

Novel highly selective peroxisome proliferator-activated receptor δ (PPARδ) modulators with pharmacokinetic properties suitable for once-daily oral dosing

Bharat Lagu [a,*], Arthur F. Kluge [a], Ross A. Fredenburg [a], Effie Tozzo [a], Ramesh S. Senaiar [b], Mahaboobi Jaleel [b], Sunil K. Panigrahi [b], Nirbhay K. Tiwari [b], Narasimha R. Krishnamurthy [b], Taisuke Takahashi [c], Michael A. Patane [a]

[a] Mitobridge, Inc., 1030 Massachusetts Ave., Cambridge, MA 02138, United States
[b] Aurigene Discovery Technologies, Ltd., Hyderabad and Bengaluru, India
[c] Astellas Pharma, Tsukuba, Japan

ARTICLE INFO

Article history:
Received 21 August 2017
Revised 26 September 2017
Accepted 18 October 2017
Available online 27 October 2017

Keywords:
PPARδ modulator
GW501516
Plasma exposure
Ligand binding domain
X-ray structure

ABSTRACT

Optimization of benzamide PPARδ modulator **1** led to (*E*)-6-(2-((4-(furan-2-yl)-*N*-methylbenzamido) methyl)phenoxy)-4-methylhex-4-enoic acid (**18**), a potent selective PPARδ modulator with significantly improved exposure in multiple species following oral administration.

Three known isoforms of a family of nuclear receptors called peroxisome proliferator-activated receptors (PPARs) manage the biosynthesis, oxidation, transport and storage of lipids by governing gene regulation of mRNAs responsible for proteins that coordinate these activities.[1] Modulators of PPARα (fibrates) and PPARγ (thiazolidinones) have been approved as treatments for dyslipidemia and diabetes, respectively. PPARδ is highly expressed in liver, skeletal muscle, intestine and adipose tissue.[2] Therefore, selective PPARδ modulators could potentially be useful treatments for metabolic disorders and conditions that would benefit from muscle regeneration.[3,4]

Recently, Evans and co-workers have disclosed a chemical series of potent selective PPARδ modulators, such as compound **1** (Fig. 1)[5] which are structurally distinct from the known PPARδ modulator, GW501516.[6] Herein, we describe structural modifications of **1** that were intended to improve exposure following oral dosing. This effort culminated in the identification of a potent and selective PPARδ modulator, compound **18**, which is suitable for further *in vivo* characterization.

Compound **1** was found to have high clearance in mice and served as a starting point for medicinal chemistry.[7,8] We modified regions of its structure based on *in vivo* metabolism studies and PPARδ receptor data. Through iterative optimization using structure-activity relationships (SAR), compound **18** was identified; it displayed significantly improved *in vivo* exposure (following i.v. and p.o. dosing) when compared to compound **1**. The SAR, pharmacokinetic data in multiple species and the protein bound X-ray structure of **18** are presented.

A general synthesis for the compounds in Table 1 is shown in Scheme 1.[9] Reductive amination of salicylaldehyde with methylamine hydrochloride provided 2-((methylamino)methyl)phenol **2**. Suzuki coupling of iodobenzoic acid with furan-2-yl boronic acid produced 4-(furan-2-yl)benzoic acid **3**. The coupling of **2** and **3** led to amide **4**, which after alkylation reaction with a 6-bromohexanoic ester or a 6-bromohexenoic ester **5** yielded the corresponding ester **6**. Hydrolysis of these esters formed the corresponding carboxylic acids **7**–**18**.

As shown in Fig. 2, the benzamide series as exemplified by the structure of compound **1** has been divided into three regions ("head", "core" and "tail") for discussion purpose. Oral dosing of **1** in mice revealed that the clearance rate of **1** (195 mL/min/kg)

* Corresponding author.
E-mail address: blagu@mitobridge.com (B. Lagu).

https://doi.org/10.1016/j.bmcl.2017.10.037
0960-894X/

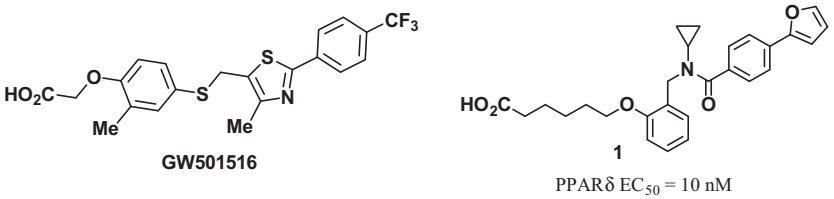

Fig. 1. PPARδ modulators.

Table 1
SAR for PPARδ activity and i.v. exposure data from studies with CD-1 mice.

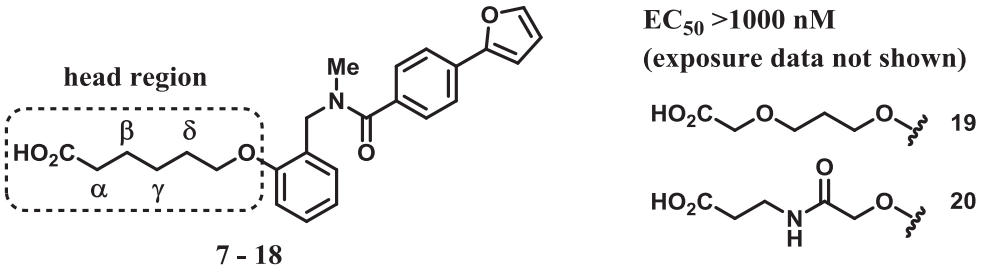

Cpd	"Head" Region Modification	PPARδ EC_{50} (nM)[a]	PPARδ EC_{50} (nM)[b]	$t_{½}$ (h)[c]	CL (mL/min/kg)	AUC (ng*h/mL)
7	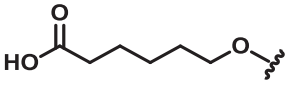	13	47	1.7	44	1100
8	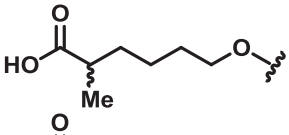	230	640	2.8	3	11,400
9	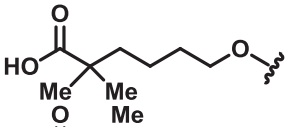	510	>10,000	4.6	1.3	48,400
10	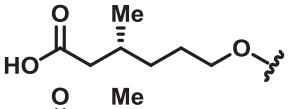	270	417	3.9	0.3	77,700
11	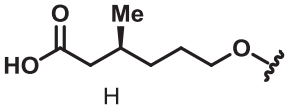	>10,000	>10,000	2.0	1.3	30,800
12[d]	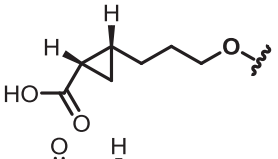	270	330 ± 10	2.7	1.7	30,100
13[d]	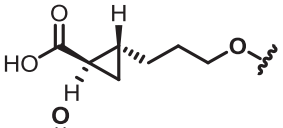	210	1630 ± 880	3.5	0.6	40,500
14	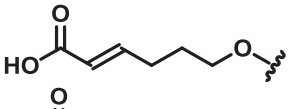	80	NA	1.9	67	750
15	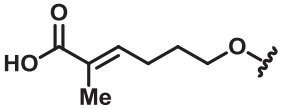	1850	>10,000	1.2	4	1300
16	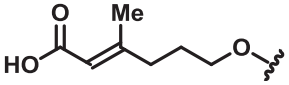	690	>10,000	1.6	11	4700

(*continued on next page*)

Table 1 (*continued*)

Cpd	"Head" Region Modification	PPARδ EC_{50} (nM)[a]	PPARδ EC_{50} (nM)[b]	$t_{½}$ (h)[c]	CL (mL/min/kg)	AUC (ng*h/mL)
17	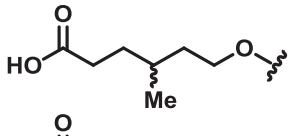	40	990	1.7	4	11,800
18	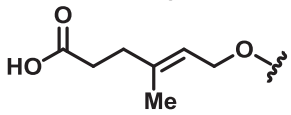	5	37 ± 5	2.3	15	3300

The numbers are n = 1 unless SEM is shown.
[a] Protein interaction assay.
[b] Transactivation assay.
[c] Compounds dosed at 3 mg/kg.
[d] Relative stereochemistry determined by ^{1}H NMR for racemic compound. NA = Not Available.

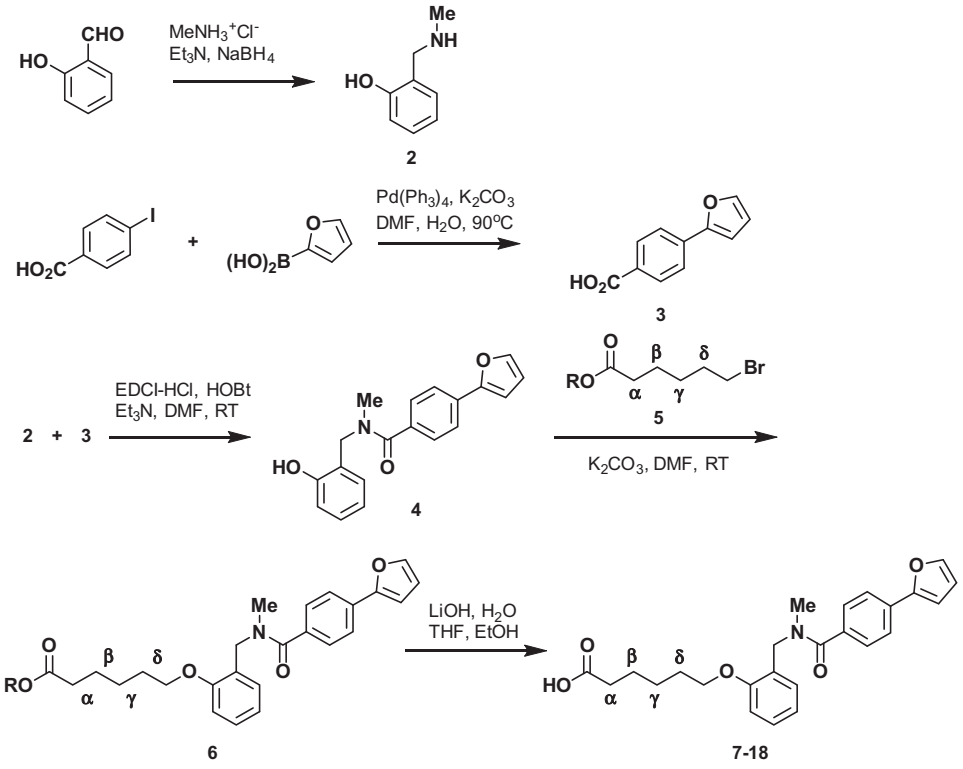

Scheme 1. General synthesis of compounds in Table 1.

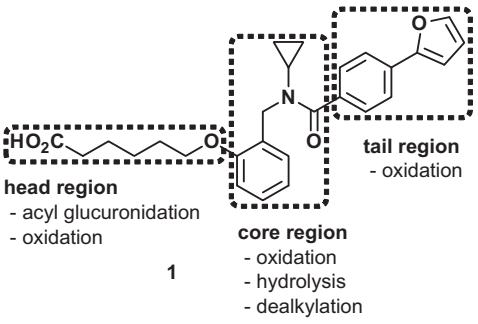

Fig. 2. Sites for Phase I and Phase II metabolism of **1**.

exceeded the rate of mouse hepatic blood flow (90 mL/min/kg).[10,11] Therefore, **1** was unsuitable for *in vivo* mouse efficacy studies and further optimization was necessary to identify a better candidate for pharmacological evaluation. Incubation of **1** with rat liver microsomes revealed multiple metabolic sites (Fig. 2) that included oxidation in the aromatic groups in the "tail" and "core" region, N-dealkylation and hydrolysis of the amide bond. Incubation of other compounds in this series with rat and human hepatocytes showed acyl glucoronidation as a route for metabolism.[12] Noticing that the trend for clearance rate was similar in rat and mouse, we screened the new analogs for mouse i.v. exposure.[13] Later, plasma exposure following oral and i.v. dosing in mice and rats were measured for the more interesting compounds.

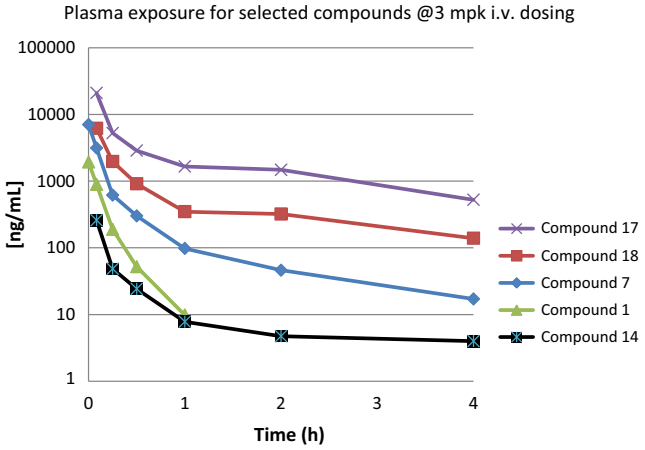

Fig. 3. Plasma exposure for compounds with EC_{50} <100 nM after 3 mg/kg i.v. dosing in CD-1 mice.

We initially attempted to decrease clearance by modifying the furan in the "tail" region or the phenyl group in the "core" region (Fig. 2) by: 1) introducing substituents on the aryl rings and 2) replacing the furan ring with cyclopropylethynyl, trifluoromethylethynyl and 4-trifluoromethoxyphenyl groups. However, while these analogs maintained PPARδ potency (data not shown), the clearance rate was unaffected. Serendipitously, we discovered that the *N*-methyl amide, compound **7**, had a decreased clearance rate compared to the clearance rate for **1** (44 mL/min/kg versus 195 mL/min/kg) after i.v. dosing in mice. Based on this finding, we kept the *N*-methyl amide and the 2-furyl group ("tail" region) constant and systematically modified the "core" and "head" regions. While the "core" region modifications did not affect the clearance rate (data not shown), the "head" region modifications significantly improved the PK properties of the series. The results are summarized in Table 1.

The PPARδ potency was determined in two assays, a protein interaction assay[14] and a trans-activation assay.[15] Typically lower EC_{50} numbers (2–8-fold) were obtained in the protein interaction assay as compared to the trans-activation assay, but the rank order of activities was similar in both assays. Compounds **19** and **20** contain etheryl and amido linkers, which was associated with loss of PPARδ activity and suggests that there is a lack of tolerance for polar groups in the "head" region. Therefore, non-polar groups

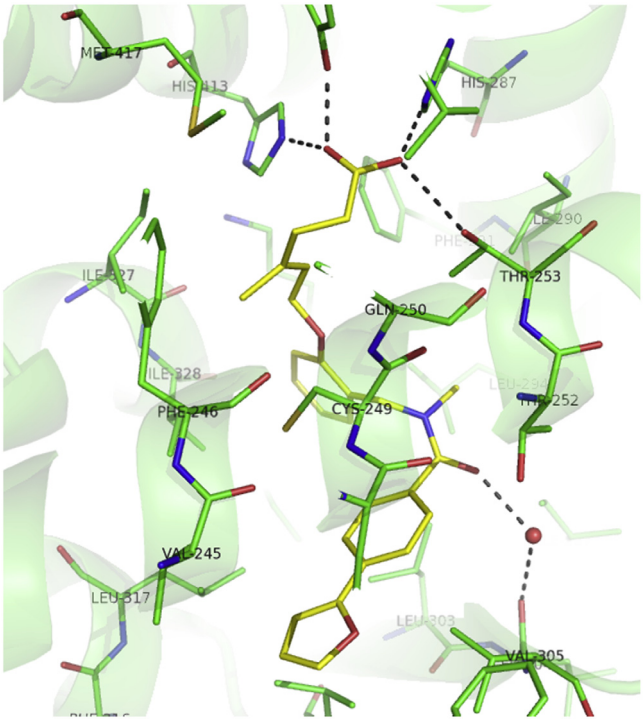

Fig. 4. X-ray structure of compound **18** (yellow) bound to LBD of PPARδ.

were incorporated at the α, β, γ or δ positions of the hexanoic acid "head" region in the subsequent analogs. Analogs with substitution at the α and β positions of the carboxylic acid (**8**–**13**) displayed significantly improved half-lives, clearances and exposures. This observation may be related to the impact of these substituents on β-oxidation and/or glucuronide formation of the carboxylic acid, which could be principle component(s) of the high clearance observed for this series. However, the improvements in the PK parameters for **8**–**13** came with diminished PPARδ potency compared to **7**. One analog, the α,β-unsaturated compound **14**, showed only 6-fold loss in PPARδ potency as compared to **7**. The methyl substituent on the double bond at α or β position was associated with improved clearance and exposure values for compounds **15** and **16**; however, these analogs also exhibited significantly lower PPARδ potency. Incorporating a methyl group in the γ-position

Table 2
Potency, selectivity, ADME, DMPK, and PK data for **18**.

Assay	Results
Human PPARδ	EC_{50} = 5 nM[a]; EC_{50} = 37 ± 5 nM[b]
Human PPARα	EC_{50} >10,000 nM[a]; EC_{50} = 6100 nM[b]
Human PPARγ	EC_{50} >10,000 nM[a,b]
Direct binding to hPPARδ by SPR[16]	K_D = 57 ± 1 nM
Thermodynamic solubility	190 μM
Caco-2 permeability	A to B = 4.58E−05; B to A = 1.03E−04 (Efflux ratio 2.24)
CYP450 inhibition	>10 μM for CYPs 3A4, 2C9, 2C19, 2D6, 1A2
Mouse PK[c]	**1 mg/kg IV:** t½ = 5.8 h; CL = 8.4 mL/min/kg; Vss = 2.6 L/kg; AUC = 1980 ng*h/mL
	10 mg/kg PO: t½ = 4.3 h; Cmax = 11,100 ng/mL; AUC = 16,600 ng*h/mL; %F = 84
Rat PK[d]	**3 mg/kg IV:** t½ = 4.5 h; Vss = 0.9 L/kg; CL = 7.2 mL/min/kg; AUC = 4650 ng*h/mL
	10 mg/kg PO: t½ = 2.5 h; Cmax = 3805 ng/mL; AUC = 12,500 ng*h/mL;%F = 82
Monkey PK[e]	**3 mg/kg IV:** t½ = 1.8 h; CL = 8 mL/min/kg; Vss = 1.3 L/kg; AUC = 6200 ng*h/mL
	10 mg/kg PO: t½ = 1.1 h: Cmax = 4190 ng/mL; AUC = 6050 ng*h/mL; %F = 29

[a] Protein interaction assay.
[b] Transactivation assay.
[c] Male CD1 mice (n = 3).
[d] Male Wistar rats (n = 3).
[e] Male cynomolgus monkeys (n = 3).

led to **17**, which showed significantly reduced clearance and improved exposure with a small loss in PPARδ potency. Compound **18**, which combined the γ-methyl group and a γ,δ *trans* double bond maintained PPARδ activity and improving clearance and exposure. The plasma exposure after intravenous dosing in mice for all the compounds with EC_{50} under 100 nM are illustrated graphically in Fig. 3.

Thus, compound **18** became a pivotal compound for the program and was profiled in more detail as summarized in Table 2. Compound **18** displayed good ADME profile and good exposure in mice, rats and monkeys following oral dosing.

An X-ray crystal structure of **18** bound to the ligand binding domain (LBD) of the hPPARδ receptor was obtained with resolution of 2.0 Å.[17] Compound **18** was tightly integrated with various amino acids throughout the LBD, totaling a series of twenty contacts with residues within 4 Å. As shown in Fig. 4, it formed H-bond interactions of its carboxylic acid with side chains of His287, His413, Thr253 and Tyr437, and proceeded to curl around helix 3 similar to the reported structure of **1**.[5] The benzamide carbonyl was observed to be 34° out of the plane of the benzene ring. However, it appears that loss of conjugation with the benzene might have been compensated for by a hydrogen bonding interaction of the carbonyl oxygen with a water molecule that mediated interactions between it and the carbonyl of Leu304. Additional hydrophobic contacts were seen with hydrophobic residues such as Leu294, Phe291, Leu303, and Leu304. The hydrophobic contacts with Val245, Val305, Val312, Phe316 and Leu317 were strong at the entrance of the Y-shaped binding pocket near the furan moiety.

In summary, we successfully optimized the pharmacokinetic properties of the benzamide carboxylic acid PPARδ modulator **1**, which led to identification of compound **18**. The *in vivo* efficacy, gene regulation profile and safety studies for **18** are discussed in an accompanying paper.[18] The protein bound structure of **18** enabled further refinements of the structure and properties of **18**, which will be presented in due course.

Acknowledgements

The authors thank Drs Masanori Miura and Susumu Watanuki (Astellas Pharma), Susanta Samajdar and Chetan Pandit (Aurigene) for helpful discussions.

References

1. Pirat C, Farce A, Lebègue N, et al. *J Med Chem*. 2012;55:4027.
2. Girroir EE, Hollingshead HE, He P, Zhu B, Perdew GH, Peters JM. *Biochem Biophys Res Commun*. 2008;371:456.
3. Barish GD, Narkar VA, Evans RM. *J Clin Invest*. 2006;116:590.
4. Fan W, Waizenegger W, Lin CS, et al. *Cell Metab*. 2017;25:1186.
5. Wu C-C, Baiga TJ, Downes M, et al. *Proc Natl Acad Sci USA*. 2017;114:E2563.
6. Oliver Jr WR, Shenk JL, Snaith MR, et al. *Proc Natl Acad Sci USA*. 2001;98:5306.
7. The maximum rate for clearance/extinction of a drug given i.v. to a mouse is the cardiac output (CO), which is approximately 500 mL/min/kg: see Janssen B, Debets J, Leenders P, Smits J. *Am J Physiol*. 2002;282:R928.
8. In this letter plasma clearance (CL) is categorized as high, medium or low with respect to its percentage of total CO. Clearance is ranked as high if it is above 0.35 CO, medium if it is around 0.15 CO and low if it is around 0.05 CO: see Toutain PL, Bousquet-Melou A. *J Vet Pharmacol Ther*. 2004;27:415.
9. Detailed synthetic schemes and procedures for preparing the compounds described in this letter can be found in PCT Int. Appl. WO 2016057660.
10. Davies B, Morris T. *Pharm Res*. 1993;10:1093.
11. All the animal experiments were carried out as per the guidelines of the Committee for the Purpose of Control and Supervision of Experiments on Animals (CPCSEA), Government of India and approved by the Institutional Animal Ethics Committee (IAEC), Aurigene Discovery Technologies Ltd, Bengaluru, India.
12. Compound (10 mmol/L) was incubated with cryopreserved rat (male and female) and human (gender mixed) hepatocytes (1×10^6 cells/mL) at 37 °C in for 30 and 120 min. The metabolites were analyzed by LC–MS. The authors thank Dr. Keitarou Kadono (Astellas Pharma) for the data.
13. Compounds were dosed as a solution in 2% DMA, 20% HPβCD intravenously at 3 mg/kg to male CD-1 mice. A standard elimination curve was generated by measuring plasma exposure at 10 points between 0 and 24 h. The values shown are an average of three determinations at each time point.
14. In the protein interaction assay the PPAR ligand complexes with a PPAR ligand binding domain fused to an inactive fragment of galactosidase. This complex complements another inactive galactosidase fragment to form an active galactosidase enzyme that is read out in a fluorescence assay. See www.discoverx.com for details. All the compounds in Table 1 were inactive (EC_{50} >10,000 nM) as modulators of PPARα and PPAR γ. Compound **1**, with a mean EC_{50} of 9.8 ± 2.5 nM, served as a positive control for PPARδ in each run.
15. In the transactivation assay CV-1 cells are transfected with a PPAR ligand binding domain fused to a GAL4 promoter to generate a hormone-inducible activator. A test ligand is added and activity is measured in a luciferase assay. See WO2016057660 for further details.
16. SPR binding studies were performed with PPARδ His-tagged (33.2 kD) at 25 °C using a one-shot kinetics approach. BioRad ProteOn XPR36 optical biosensor equipped with a nickel-charged, NTA-derivatized GLH sensor chip and equilibrated with running buffer (10 mM HEPES, 150 mM NaCl, 5% glycerol, 1 mM TCEP, 0.005% Tween-20, pH 7.5) was used for analysis.
17. Coordinates of the X-ray structure have been deposited in the Protein Data Bank (accession code PDB 5XMX). The residue numbering follows the UniProt residue numbering convention in accession number Q03181 (PPARD_HUMAN).
18. Lagu B, Kluge AF, Goddeeris MM, et al. *Bioorg Med Chem Lett*. 2017 (accompanying paper).